Immunity
Article

Omental Milky Spots Develop in the Absence of Lymphoid Tissue-Inducer Cells and Support B and T Cell Responses to Peritoneal Antigens

Javier Rangel-Moreno,[1,3] Juan E. Moyron-Quiroz,[2,3] Damian M. Carragher,[2] Kim Kusser,[1] Louise Hartson,[1] Amy Moquin,[2] and Troy D. Randall[1,*]
[1]Division of Allergy, Immunology and Rheumatology, University of Rochester, Rochester, NY 14642, USA
[2]Trudeau Institute, Saranac Lake, NY 12983, USA
[3]These authors contributed equally to this work
*Correspondence: troy_randall@urmc.rochester.edu
DOI 10.1016/j.immuni.2009.03.014

SUMMARY

The omentum is a site of B1 cell lymphopoiesis and immune responsiveness to T cell-independent antigens. However, it is unknown whether it supports immune responses independently of conventional lymphoid organs. We showed that the omentum collected antigens and cells from the peritoneal cavity and supported T cell-dependent B cell responses, including isotype switching, somatic hypermutation, and limited affinity maturation, despite the lack of identifiable follicular dendritic cells. The omentum also supported $CD4^+$ and $CD8^+$ T cell responses to peritoneal antigens and recruited effector T cells primed in other locations. Unlike conventional lymphoid organs, milky spots in the omentum developed in the absence of lymphoid tissue-inducer cells, but required the chemokine CXCL13. Although the lymphoid architecture of milky spots was disrupted in lymphotoxin-deficient mice, normal architecture was restored by reconstitution with lymphotoxin-sufficient hematopoietic cells. These results indicate that the milky spots of the omentum function as unique secondary lymphoid organs that promote immunity to peritoneal antigens.

INTRODUCTION

The omentum is a fatty tissue that connects the spleen, stomach, pancreas, and colon (Williams and White, 1986) and often occludes wounds in the peritoneal cavity, including hernias, inflamed appendices, tumors, and other infected or inflamed sites (Morrison, 1906). Surgeons appreciate the immunological and wound-healing properties of the omentum and take advantage of these properties in reconstructive procedures or to close large surgical incisions (Williams and White, 1986). The advantages of the omentum for surgical closure include its enormous angiogenic potential (Goldsmith et al., 1984), large surface area (Das, 1976), and apparent immunological activity (Roberts, 1955; Walker and Rogers, 1961).

The omentum contains milky spots (MSs), which are clusters of leukocytes embedded in the omental tissue (Krist et al., 1995a). The MSs also collect fluids, particulates, and cells from the peritoneal cavity (Fedorko et al., 1971; Gerber et al., 2006; Hodel, 1970), and the frequency and size of MSs increase in the omenta of patients undergoing peritoneal dialysis (Beelen et al., 2005; Di Paolo et al., 2005). Plasma cell responses to some T cell-dependent antigens are observed in the omenta of mice immunized i.p. (Dux et al., 1977, 1986; Hajdu et al., 1972), and the surgical removal of the omentum in rabbits reduces the antibody response to i.p. SRBC by 75% (Portis, 1924), suggesting that the MSs may be secondary lymphoid organs. However, the MSs of naive animals consist primarily of macrophages and B1 cells, with few T cells (Beelen et al., 1980; Krist et al., 1995b; Van Vugt et al., 1996). Because they also seem to lack interdigitating dendritic cells and follicular dendritic cells (FDCs) (Van Vugt et al., 1996), and because some studies were unable to elicit T cell-dependent immune responses in the omentum (Szaniawska, 1974, 1975), some investigators conclude that MSs are not true secondary lymphoid tissues (Szaniawska, 1974, 1975; Van Vugt et al., 1996). Moreover, even in studies showing omental plasma cell responses, it is unclear whether these cells were originally primed in the omentum or in other secondary lymphoid organs. Thus, the immunological function of the MSs is unclear.

Other data indicate that B1 cells initially develop from hematopoietic progenitors in the fetal omentum and fetal liver and are then maintained by a process of self-renewal in the peritoneal cavity (Solvason et al., 1992; Solvason and Kearney, 1992). In fact, the leukocytes in the MSs are similar in composition to those in the peritoneal cavity, with a predominance of B1 cells and macrophages (Ansel et al., 2002; Beelen et al., 1980). Importantly, B1 cells express a unique repertoire of antigen receptors, including the T15 idiotype, which recognizes phosphorylcholine, a cell surface component of some bacteria (Benedict and Kearney, 1999; Vakil et al., 1991). Intestinal leakage or the intraperitoneal delivery of bacteria leads to rapid activation of B1 cells and promotes T cell-independent antibody responses (Ansel et al., 2002; Ha et al., 2006). Moreover, cells in the MSs are highly responsive to bacterial products like LPS (Cui et al., 2002; Ha et al., 2006), suggesting that B1 cells in the peritoneal cavity and omentum are specialized to provide natural immunity to bacterial pathogens. Consistent with this idea, *Cxcl13*$^{-/-}$ mice make poor

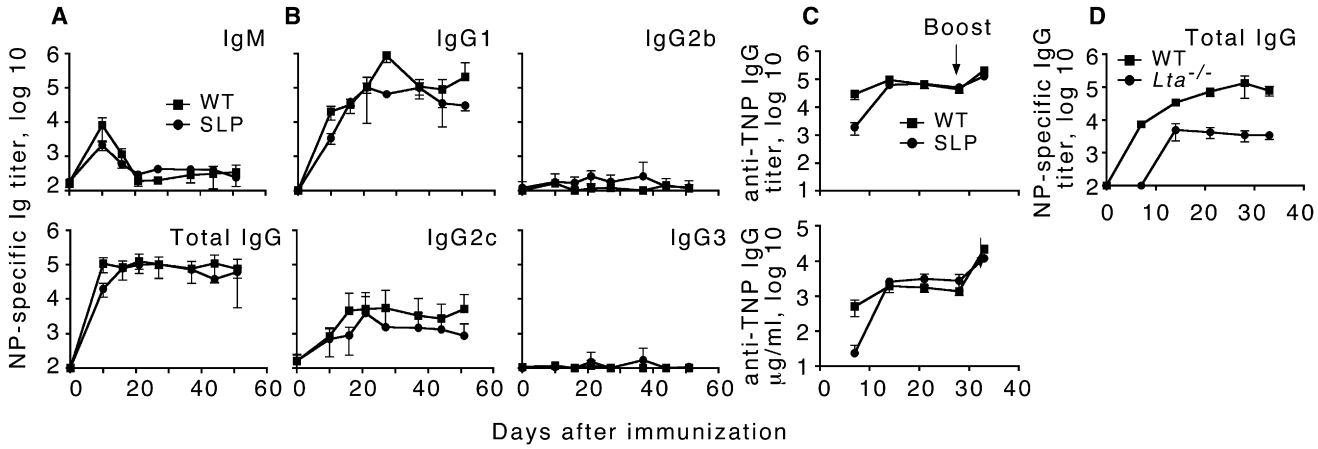

Figure 1. Antibody Responses to Peritoneal Antigens in the Absence of Conventional Lymphoid Organs

(A and B) WT and SLP mice were i.p. immunized with NP-OVA. The serum titers of NP-specific IgM and total IgG (A) as well as NP-specific IgG1, IgG2a, IgG2b, and IgG3 (B) were determined by ELISA. This experiment is representative of two experiments with five mice in each group.

(C) WT and SLP mice were immunized with TNP-KLH. The serum titers of TNP-specific IgG were determined by ELISA and the concentration of TNP-specific IgG was determined by comparison to a monoclonal anti-TNP standard. This experiment was performed twice with similar results.

(D) C57BL/6 and splenectomized *Lta*$^{-/-}$ mice were immunized with NP-OVA. The serum titers of NP-specific IgG were determined by ELISA.

antibody responses to bacterial antigens in the peritoneal cavity and have low titers of natural antibody, including the T15 idiotype (Ansel et al., 2002). Thus, the cell types in the peritoneal cavity and omentum appear specialized to provide innate immunity to T cell-independent bacterial antigens.

Despite the immunological potential of the MSs, many investigators use intraperitoneal injection to immunize laboratory mice with T cell-dependent antigens and then assay those responses in the spleen or perithymic lymph nodes (LNs)—ignoring any possible role for the omentum. More importantly, the MSs of the omentum collect metastasizing tumor cells (Gerber et al., 2006; Krist et al., 1998), fluid from peritoneal dialysis (Beelen et al., 2005), bacteria from intestinal perforations (Ha et al., 2006), and antigens from abdominal injuries (Morrison, 1906)—particularly when the omental tissue is used in reconstructive surgeries (Williams and White, 1986). Thus, it is essential that we understand the immunological properties of the MSs.

Here we tested whether the MSs of the omentum were formed by the same developmental pathways used by conventional lymphoid organs and whether they could independently support immune responses to peritoneal antigens. We found that, unlike conventional lymphoid organs, MSs developed in the absence of lymphoid tissue-inducer cells, but required the chemokine CXCL13. Although the lymphoid architecture of milky spots was disrupted in lymphotoxin (LT)-deficient mice, normal architecture could be restored by reconstitution with LT-sufficient hematopoietic cells. We also found that MSs lacked networks of follicular dendritic cells; however, they were capable of supporting T cell-dependent B cell responses, including isotype switching, somatic hypermutation, and limited affinity maturation. The omentum also supported $CD4^+$ and $CD8^+$ T cell responses to peritoneal antigens and recruited effector T cells primed in other locations. These results indicate that the milky spots of the omentum function as unique secondary lymphoid organs that promote immunity to peritoneal antigens.

RESULTS

Mice Lacking Conventional Lymphoid Organs Generate B Cell Responses to Peritoneal Antigens

To test whether functional local lymphoid tissues were formed in response to antigenic challenge in the peritoneal cavity, we intraperitoneally (i.p.) immunized wild-type (WT) as well as spleen lymph node and Peyer's patch-deficient (SLP) mice with (4-hydroxy-3-nitrophenyl)-acetyl(15)-OVA (NP-OVA) adsorbed to alum and measured the serum titers of NP-specific antibody. We found that WT and SLP mice produced similar titers of NP-specific IgM that peaked early after immunization and were subsequently maintained at low amounts (Figure 1A). The titers of NP-specific total IgG rapidly increased in both WT and SLP mice and stayed very high for nearly 2 months after immunization (Figure 1A). Both WT and SLP mice predominantly generated NP-specific IgG1 and to a lesser extent IgG2a (Figure 1B). Very little IgG2b or IgG3 were observed in either WT or SLP mice.

We also immunized WT and SLP mice with 2,4,6-trinitrophenyl(30)-KLH (TNP-KLH) adsorbed to alum and boosted the mice on day 28. As observed in the previous experiment, the SLP mice were slower to generate antigen-specific IgG, but the titers were equivalent by day 14 after immunization (Figure 1C). In addition, the titers of TNP-specific IgG rapidly increased after the booster immunization in both groups (Figure 1C). Because IgG titers do not give a good sense of how much antigen-specific IgG was produced, we repeated the ELISAs with anti-TNP standards and found that the SLP mice were slow to generate high titers of anti-TNP IgG, but that both groups ultimately generated more than 1 mg/ml of serum anti-TNP IgG. Together, these data demonstrate that conventional lymphoid organs—spleen, LNs, and Peyer's patches—are not necessary for B cell responses to haptenated proteins in the peritoneal cavity.

We were initially surprised that SLP mice made such a robust antibody response to NP-OVA, given that lymphotoxin-deficient

($Lta^{-/-}$) mice make such poor antibody responses to peritoneal antigens (Banks et al., 1995; Matsumoto et al., 1996b) because of their lack of lymph nodes and disrupted splenic architecture (Banks et al., 1995; de Togni et al., 1994). To reconcile our data with published results, we i.p. immunized C57BL/6 and splenectomized $Lta^{-/-}$ mice with NP-OVA adsorbed to alum and measured the titers of NP-specific IgG. We found that the IgG response in splenectomized $Lta^{-/-}$ mice was both delayed and significantly ($p < 0.01$) reduced compared to that in C57BL/6 mice (Figure 1D). Because both SLP and splenectomized $Lta^{-/-}$ mice lack spleen and lymph nodes, we conclude that the major immune defect in $Lta^{-/-}$ mice is due to the loss of LTα, rather than the loss of spleen and lymph nodes.

The Lymphoid Areas of the Omentum Exhibit Characteristics of Secondary Lymphoid Organs

Although spleen and lymph nodes are absent from SLP mice, it was possible that local lymphoid tissues, such as MSs, remained that could be responsible for generating antibody responses to peritoneal antigens. To test whether MSs were present in the omentum of naive SLP mice, we examined whole mounts of omentum. We found MSs that consisted of large clusters of B cells with PNAd-expressing vessels in the omenta of both WT and SLP chimeric mice (Figures 2A and 2B). To test whether the MSs collected haptenated OVA, we injected OVA labeled with Alexa Fluor 594 into the peritoneal cavity and examined the MSs by immunofluorescence. We found that labeled OVA was easily detected in the MSs as early as 2 hr after injection (Figure 2C) and was highly concentrated by 4 hr after injection (Figure 2D).

To determine whether particulates in the peritoneal cavity were actively carried to the MSs via phagocytic cells or were passively collected, we next transferred CFSE-labeled SRBCs to the peritoneal cavity. We found that peritoneal SRBCs rapidly collected in the MSs (Figure 2E). At higher magnification, it was clear that many of the CFSE-labeled SRBCs had been engulfed by CD11b-expressing phagocytic cells (Figure 2E, arrows). Flow cytometry revealed that the majority of SRBCs in the omentum were internalized by phagocytic cells (Figure 2F) although a small proportion of SRBCs were not associated with other cells (Figure 2F, gated population). The SRBC transfer also changed the composition and cellularity of the omentum (Figure 2G), with the largest increase in cell frequency occurring in the $CD11c^{-}CD11b^{hi}$ population (Figure 2G, box E). The total number of cells in the omentum increased about 4-fold upon SRBC administration, with significant increases ($p < 0.05$) occurring in all cell populations—even the lymphocyte population (Figure 2G, box C), which was the only population that did not phagocytose SRBCs (Figure S1 available online). These data confirm previous reports that activation of peritoneal cells promotes their migration to the omentum (Ha et al., 2006) and demonstrate that at least some particulates can be passively collected by the omentum in addition to being captured by phagocytic cells.

To further test the idea that there is bulk flow from the peritoneal cavity through the MSs, we injected EL4 lymphoma cells that had been transfected with green fluorescent protein (GFP). We found that EL4-GFP cells rapidly accumulated in the omentum (Figure 2I) and were found in close association with B cells in the MSs (Figure 2J). This accumulation was largely unaffected by pretreatment with pertussis toxin (PTX) (Figures 2I and 2J), although there was a small decrease in the frequency and number of PTX-treated EL4 cells that accumulated in the omentum (Figures 2K and 2L). To test whether this was also true of lymphocytes, we purified B cells from green fluorescent protein (GFP) transgenic mice and purified T cells from C57BL/6 mice, which we labeled with BODIPY 558-568. These cells were mixed, incubated with or without PTX, and injected into the peritoneal cavity. We found that whereas B and T cells accumulated in the omentum regardless of whether they were pretreated with PTX, the untreated cells rapidly entered MSs and segregated into B and T cell areas (Figure 2M). In contrast, cells pretreated with PTX collected in the omentum, but the B and T cells were scattered and did not form compact follicular structures. As with the EL4 cells, the frequency and number of lymphocytes that migrated to the omentum was reduced by PTX treatment (Figures 2N and 2O). Thus, peritoneal cells clearly use PTX-sensitive mechanisms to actively migrate to the omentum, but can also accumulate in the omentum by other mechanisms. However, the segregation of B and T cells and the formation of follicular structures in the MSs are controlled by PTX-sensitive mechanisms.

Milky Spots Support T Cell-Dependent Immune Responses to Peritoneal Antigens

Because peritoneal antigens and cells rapidly collected in the MSs, we next wanted to test whether the MSs supported immune responses to T cell-dependent antigens. Therefore, we i.p. immunized WT and SLP mice with NP-OVA adsorbed to alum and examined the response of NP-specific B cells in the omentum 7 days later. By using NP-conjugated allophycocyanin to identify NP-specific B cells, we found that both WT and SLP mice were able to generate NP-specific germinal center B cells in the omentum (Figure 3A). We also gated on B cells that were not NP specific in these same animals and found that the frequency of germinal center B cells was much lower (Figure 3B). In fact, the frequency of germinal center B cells in the NP-nonspecific B cell population was similar to that seen in omental B cells from naive mice (Figure S2). We also immunized WT and SLP mice with SRBC and boosted them on day 28. Five days after the boost, we found very high frequencies of germinal center B cells (Figure 3C) and isotype-switched plasma cells (Figure 3D) in the omenta of both groups. Although we could not demonstrate antigen specificity of these cells by flow cytometry, we found similar frequencies of SRBC-specific IgG-secreting cells in the omenta of both groups (Figure 3E) and significantly ($p < 0.01$) higher numbers of IgG-secreting cells in SLP mice (Figure 3F).

We next tested whether we could define germinal centers in MSs by histology. To examine the histology of immunized omenta, we folded individual omenta in pieces of liver, fixed them in formalin, and embedded them in paraffin. Sections of omenta embedded with this method could be easily stained with H&E to see the bluish areas of the lymphocyte-filled MSs and the lacy areas of fatty tissue surrounded by the supporting liver (Figure 3G). By using cryosections, we also found separated B and T cell areas in omenta from SRBC-immunized mice (Figure 3H), as well as clusters of IgD^{-}PNA-binding B cells (Figure 3I). In serial sections, we found that the clusters of PNA-binding B cells were also proliferating as demonstrated by PCNA expression (Figure 3J). To confirm the presence of bona fide germinal centers in the omenta of immunized mice, we also

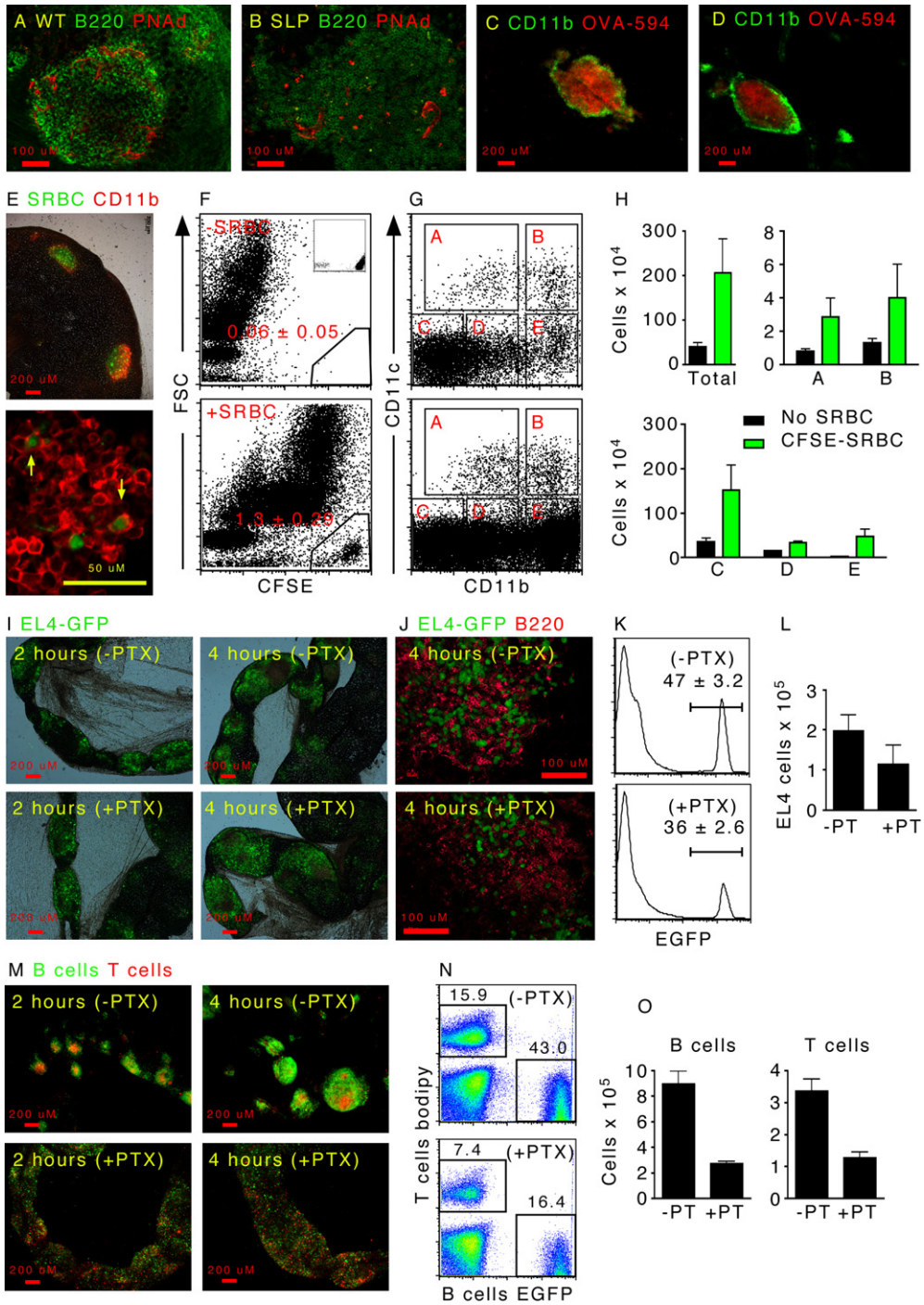

Figure 2. The Milky Spots of the Omentum Collect Peritoneal Cells and Antigens

(A and B) Omenta were obtained from naive WT and SLP mice and whole mounts were probed with antibodies to B220 and PNAd. Images were obtained as optical sections with the Zeiss Apotome.

(C and D) C57BL/6 mice were i.p. immunized with ovalbumin coupled to Alexa Fluor 594. Omenta were collected 2 or 4 hr later and whole mounts were probed with antibodies to CD11b.

(E) 1×10^6 CFSE-labeled SRBC were i.p. injected and the omenta were collected 4 hr later. Whole mounts were probed with antibodies to CD11b. The high-magnification image is an optical section obtained with the Zeiss Apotome.

(F) Omental cells from SRBC-injected and control mice were analyzed by flow cytometry. The plots show all events collected. The inset in the top panel shows the profile of CFSE-SRBC prior to injection. The numbers in each plot refer to the percentage ± standard deviation of events in the CFSE-SRBC gate.

(G) Omental cells from SRBC-injected and control mice were analyzed by flow cytometry. The plots show live leukocytes and gated into five populations based on CD11c and CD11b expression.

probed cryosections with antibodies to BCL6 (Figures 3K–3N), which is a marker of germinal center B cells (Cattoretti et al., 1995). We found clusters of $BCL6^+IgD^-$ cells surrounded by $BCL6^-IgD^+$ cells (Figures 3K and 3M). Serial sections revealed that these clusters consisted of large blast cells that expressed B220 on the cell surface and BCL6 in the nucleus (Figures 3L and 3N). These data demonstrate that the MSs support local germinal center B cell responses to peritoneal antigens.

We next tested whether CFSE-labeled OVA-specific $CD4^+$ T cells could respond in the MSs. We found that OTII cells in both WT and SLP mice immunized with alum and LPS (no OVA) predominantly expressed low amounts of CD25 (Figure 4A, top row) and high amounts of CD62L (Figure 4B, top row). In contrast, OTII cells in WT and SLP mice that were immunized with NP-OVA 36 hr previously rapidly increased their expression of CD25 and reduced their expression of CD62L (Figures 4A and 4B, middle rows). Changes in surface expression of these markers coincided with the first cell divisions of the OTII cells, although cell division was not required for either increased CD25 expression or decreased CD62L expression (Figures 4A and 4B, middle rows). OTII proliferation continued rapidly in both WT and SLP mice and most cells had divided once or twice by 42 hr after immunization (Figure 4C). We also tested whether $CD8^+$ T cells responded to NP-OVA. As shown in Figure 4D, OVA-specific $CD8^+$ T cells could be found in the MSs of both WT and SLP chimeras 7 days after immunization with NP-OVA in alum. The frequency of OVA-responding $CD8^+$ T cells was relatively low, probably because NP-OVA is an exogenous antigen that is poorly presented by cross-priming. These data demonstrate that T cell responses can also occur in the MSs of the omentum, even in mice that lack spleen, LNs, and Peyer's patches.

We next wanted to determine whether effector or memory T cell generated in other locations recirculated through the peritoneal cavity and the omentum. To test this possibility, we first intranasally infected C57BL/6 mice with influenza virus and looked in the peritoneal cavity and omentum for recirculating influenza-specific $CD8^+$ T cells. We found influenza-specific (tetramer-binding) CD8 T cells in both the peritoneal lavage and omentum of mice that had been infected with influenza 21 days previously (Figure 4E). We also orally infected IL-4 reporter (4-get) mice with larvae of the intestinal helminth *Heligmosomoides polygyrus* and looked in the peritoneal lavage and omentum for recirculating Th2 cells. Because the 4-get mice are transgenic for a reporter construct that expresses GFP under the control of the IL-4 promoter (Mohrs et al., 2001), Th2 cells should express GFP. We found GFP-expressing $CD4^+$ T cells in both the peritoneal lavage and omentum on day 28 after infection (Figure 4F). Thus, antigen-experienced $CD4^+$ and $CD8^+$ T cells recirculate through the peritoneal cavity and omentum, even when these cells were primed outside of the peritoneal cavity.

Development and Architecture of Milky Spots

We next examined the role of lymphotoxin-α (LTα) and the homeostatic chemokines CXCL13, CCL21, and CCL19 in the development and organization of the MSs. We found that the MSs were well developed in both C57BL/6 and PLT mice, which are homozygous for the *paucity of lymph node T cells* (*plt*) mutation, which inactivates the CCL19 and CCL21 genes that are expressed in secondary lymphoid organs (Nakano and Gunn, 2001). However, the MSs were much smaller or even absent in $Lta^{-/-}$ and $Cxcl13^{-/-}$ mice (Figures 5A–5C), consistent with previous observations (Ansel et al., 2002). In particular, the omenta of $Lta^{-/-}$ and $Cxcl13^{-/-}$ mice had very small or absent B cell areas and lacked detectable $PNAd^+$ HEVs (Figure 5C). Given that MSs are found in SLP mice (Figure 2B), it seems that the reconstitution of $Lta^{-/-}$ mice with normal bone marrow restores the structure of the MSs, suggesting that the defects in the MSs of $Lta^{-/-}$ mice are not due to an absolute blockade in development.

Because the MSs in the omenta of $Lta^{-/-}$ and $Cxcl13^{-/-}$ mice were architecturally abnormal, we hypothesized that LTα and CXCL13 were involved in a positive feedback loop similar to that described in other lymphoid organs (Ansel et al., 2000). To test this possibility, we extracted RNA from the omenta of naive C57BL/6, $Lta^{-/-}$, $Cxcl13^{-/-}$, and PLT mice and analyzed chemokine mRNA expression by quantitative PCR. To our surprise, we found that the expression of CXCL12, CCL21, CCL19, and CXCL13 as well as LTβ and TNF-α was essentially normal in the omentum of $Lta^{-/-}$ mice (Figure 5D). In contrast, we found that whereas the expression of CXCL12 and CCL21 was normal in the omenta of $Cxcl13^{-/-}$ mice, the expression of CCL19, CXCL13, LTβ, and TNF-α were very reduced (Figure 5D). Finally, we found that the expression of CCL19 and CCL21 was reduced in the omenta of PLT mice, consistent with the *plt* mutation, but that the expression of the other chemokines and cytokines that we tested was normal in the omentum of PLT mice (Figure 5D). These data demonstrate that even though CXCL13 is very important for the development of the MSs, its expression is not controlled by LTα.

We next tested whether the formation of the MSs required LTi cells, which are absent in mice deficient in retinoic acid related orphan receptor-γ ($Rorc^{-/-}$ mice) and in mice that lack the inhibitor of differentiation-2 ($Id2^{-/-}$ mice) (Sun et al., 2000; Yokoto et al., 1999). We found well-developed MSs with large B cell follicles in both $Rorc^{-/-}$ mice and $Id2^{-/-}$ mice (Figures 5E and 5F), suggesting that the development of MSs in the omentum occurs independently of LTi cells. Because it is possible that some types

(H) Total cells from the omenta of SRBC-injected and control mice were enumerated and the number of cells in each of the gated populations was calculated.
(I) GFP-expressing EL4 cells were cultured in vitro for 2 hr with or without pertussis toxin (PTX) and then i.p. injected into C57BL/6 recipients. Omenta were collected 2 or 4 hr later and whole mounts were examined by fluorescence microscopy.
(J) Whole mounts of omenta from EL4-GFP-injected mice were probed with B220 to visualize MSs. Images are optical sections obtained with the Zeiss Apotome.
(K) The frequency of PTX-treated and untreated EL4-GFP cells in the omenta was determined by flow cytometry.
(L) The number of PTX-treated and untreated EL4-GFP cells in the omenta was calculated. There were 4–5 mice per group.
(M) B cells were purified from GFP-transgenic mice and mixed 2:1 with purified, bodipy-labeled T cells from C57BL/6 mice. The cell mixture was cultured for 2 hr with or without PTX and 1×10^7 total cells/mouse were i.p. injected into C57BL/6 recipients. The omenta were collected 2 and 4 hr after injection and whole mounts were analyzed by fluorescence microscopy.
(N) The frequencies of PTX-treated and untreated B and T cells in the omenta were determined by flow cytometry.
(O) The numbers of PTX-treated and untreated B and T cells in the omenta were calculated. There were 4–5 mice per group.

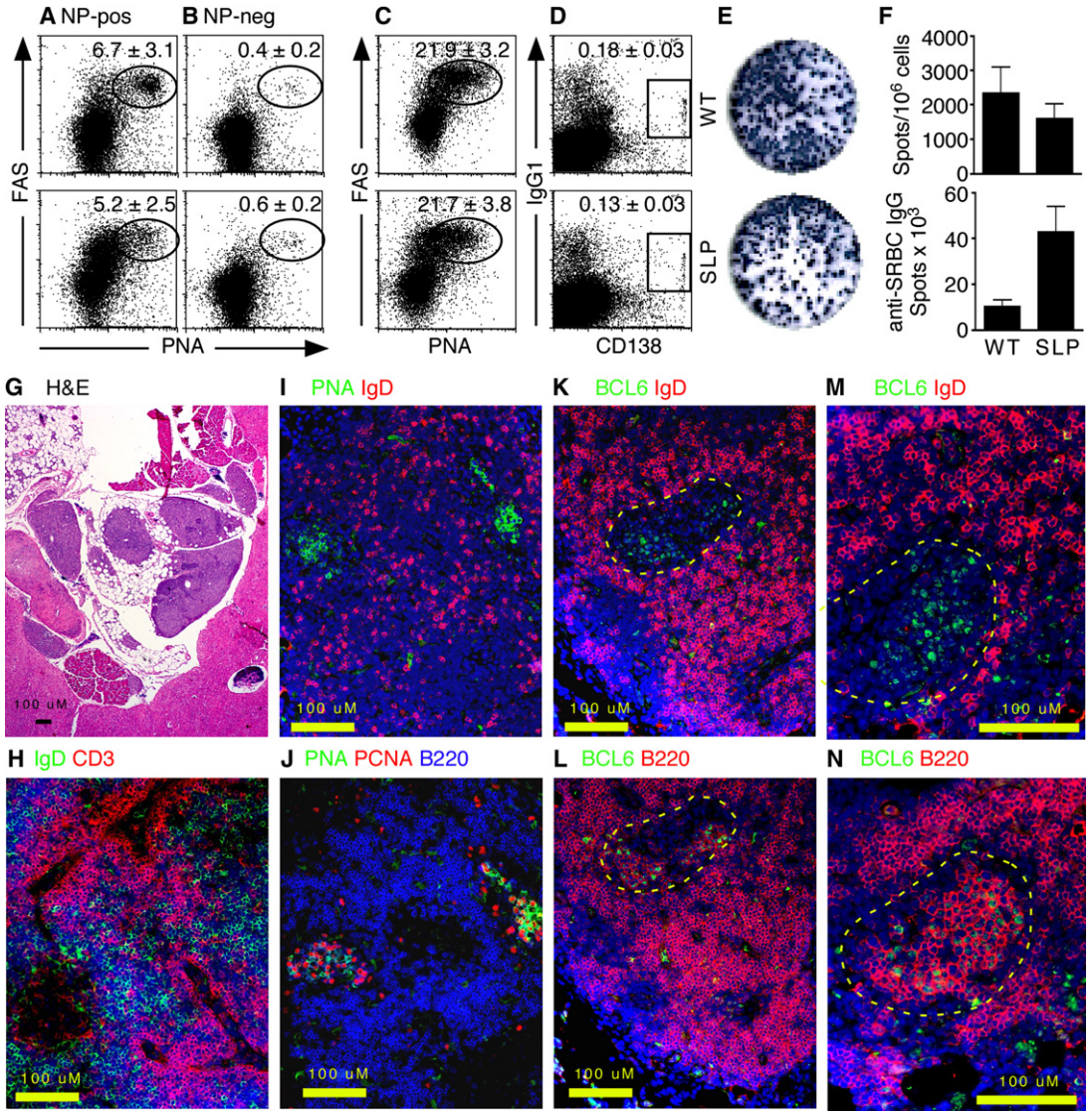

Figure 3. Antigen-Specific B Cell Responses Occur in the Omentum

(A and B) WT and SLP mice were i.p. immunized with NP-OVA and omental cells were analyzed by flow cytometry on day 8 for NP-specific FAS$^+$PNA-binding germinal center B cells (A) and NP-nonspecific FAS$^+$PNA-binding germinal center B cells (B). Cells were gated on CD19 expression and the ability to bind NP-APC (A) or the failure to bind NP-APC (B). The numbers in each plot refer to the percentage ± standard deviation of NP-specific B cells in the gates indicated by ovals or boxes.

(C and D) WT and SLP mice were i.p. immunized with SRBC and boosted on day 14, and omental cells were analyzed 5 days later by flow cytometry for FAS$^+$PNA-binding germinal center B cells (C) and IgG1$^+$CD138$^+$ plasma cells (D). Cells were gated on CD19 expression. The numbers in each plot refer to the percentage ± standard deviation of CD19$^+$ B cells in the gates indicated by ovals or boxes.

(E) WT and SLP mice were i.p. immunized with SRBC and boosted on day 14, and omental cells were analyzed by SRBC-specific ELISPOT.

(F) The frequency and total number of SRBC-specific IgG ELISPOTs was determined. There were 4–5 mice in each group.

(G) C57BL/6 mice were immunized with SRBC and omenta were collected on day 14. Omenta were embedded in pieces of liver to aid in sectioning. Paraffin sections were stained with H&E.

(H–N) C57BL/6 mice were immunized with NP-OVA and omenta were collected on day 14 and frozen in OCT. Cryosections were stained with the indicated antibodies and counterstained with DAPI (blue). Germinal centers are outlined by yellow in (K)–(N).

of LTi cells could develop in the absence of RORγ and Id2, we also looked for CD45$^+$CD4$^+$CD3$^-$ LTi cells in the developing MSs. Although we were able to identify lymphocytes in the omenta from 3-day-old pups, we did not observe IL-7Rα$^+$CD45$^+$CD4$^+$CD3$^-$ LTi cells (not shown).

Because CXCL13 was so important for the structure of the MSs, we next used immunofluorescence to examine where CXCL13 was expressed. As shown in Figure 6A, CXCL13 is primarily expressed in an area that surrounds the B cell follicle in a reticular pattern, suggesting some type of stromal cells. In fact, CXCL13 appeared to be expressed in a 3-dimensional basket that envelops the B cell area (Figure S3A). Despite the unusual pattern of CXCL13 staining, it seemed to be specific because no red signal was observed when *Cxcl13*$^{-/-}$ omenta

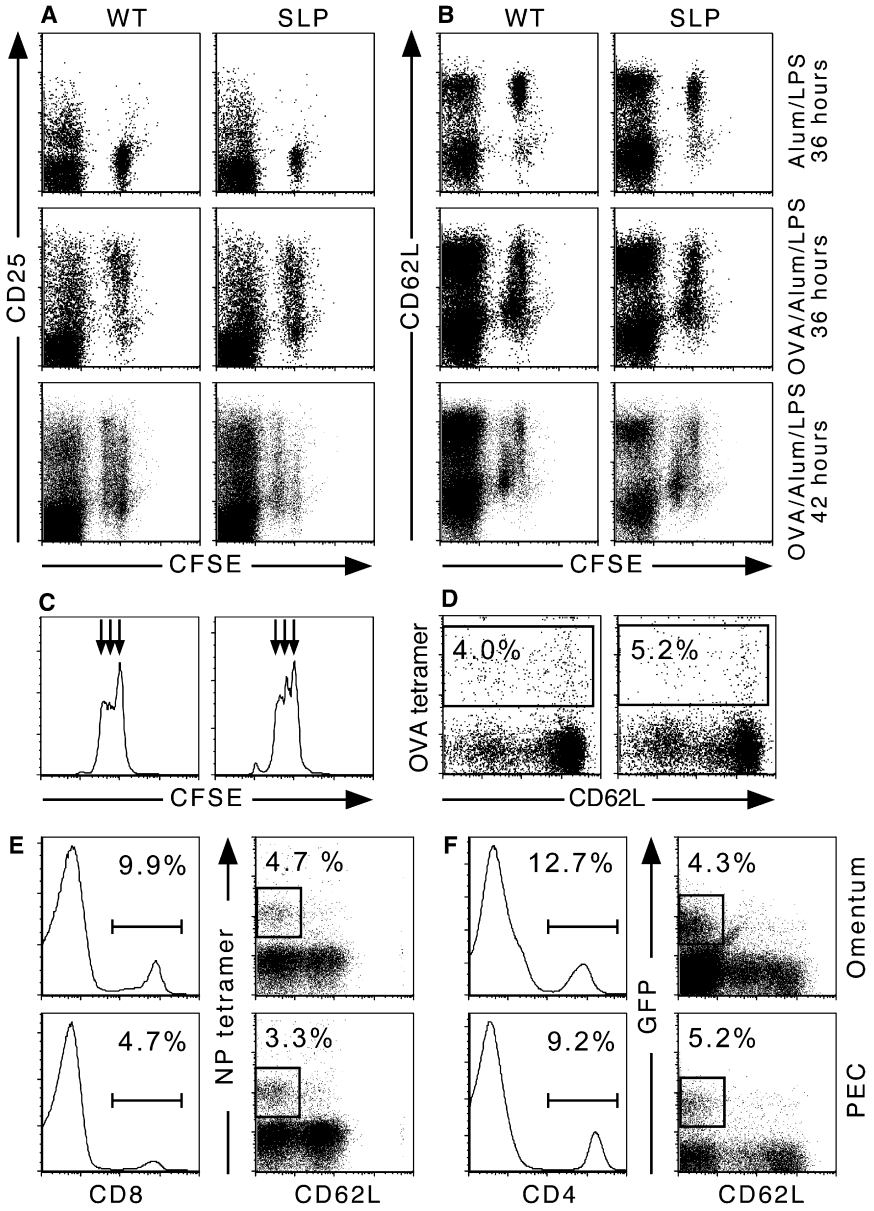

Figure 4. Antigen-Specific T Cell Responses in the Omentum

(A–C) Purified OTII CD4$^+$ T cells were labeled with CFSE and i.p. injected into WT and SLP recipient mice. Recipients were immunized 4 hr later with 100 μg OVA and 10 μg LPS adsorbed to alum or with 10 μg LPS and alum as indicated. Omenta were obtained 36 or 42 hr later and omental cells were analyzed by flow cytometry for CD4, CFSE, and CD25 (A) or CD4, CFSE, and CD62L (B). The plots shown are gated on CD4$^+$ T cells. CFSE dilution in the transferred CD4 T cells was measured by flow cytometry (C). There were 4–5 mice per group and omenta were pooled prior to analysis. The data shown are representative of three independent experiments.

(D) WT and SLP mice were immunized with 100 μg OVA and 10 μg LPS adsorbed to alum. OVA-specific CD8$^+$ T cells were identified by tetramer binding in the omenta of immunized mice. The plots shown are gated on CD8$^+$ T cells.

(E) C57BL/6 mice were intranasally infected with influenza, and single-cell suspensions from peritoneal cavity and omenta were analyzed by flow cytometry 21 days after infection. Histograms show the frequency of CD8$^+$ T cells in the live leukocyte population. Dot plots were gated on CD8$^+$ T cells and the boxes indicate influenza nucleoprotein-specific cells.

(F) 4-get IL-4 reporter mice were orally infected with *H. polygyrus* larvae, and single-cell suspensions from peritoneal cavity and omenta were analyzed by flow cytometry 28 days after infection. Histograms show the frequency of CD4$^+$ T cells in the live leukocyte population. Dot plots were gated on CD4$^+$ T cells and the boxes indicate Th2 cells based on GFP expression (B).

were stained with the same antibodies used in Figure 6A (Figure S3B). In addition, we did not observe any red signal when C57BL/6 omenta were stained with either the secondary antibody alone (Figure S3C) or with a different primary antibody followed by the secondary antibody (Figure S3D). CXCL13 expression is often associated with FDCs (Cyster et al., 2000), so we next tested whether markers of FDCs colocalized with CXCL13 via serial sections (Figures 6A–6F). We found that FDCM1 was expressed in a reticular pattern surrounding the B cell area (Figure 6B) similar to where we observed CXCL13 expression. However, we observed scattered staining only with FDCM2 (Figure 6C). Moreover, CD21 was primarily expressed on B cells and was only expressed on a few scattered non-B cells (Figure 6D). Interestingly, a few CD35-expressing cells were observed in the center of the B cell area (Figure 6E). Despite the highly unusual staining patterns of FDC markers in omentum, the same combination of antibodies used at the same time on splenic sections revealed typical staining patterns of FDCs in the center of B cell follicles (Figures 6G–6J). Despite the apparent absence of conventional FDC networks, however, we did observe a network of ERTR7$^+$ stromal cells throughout the MSs (Figure 6K). Interestingly, CD11b$^+$ macrophages, which are known to express CXCL13 in the peritoneal cavity (Ansel et al., 2002), were found around the outside of the MSs (Figures 6F and 6L), whereas CD11c$^+$ cells were found in the center of the MSs similar to where the B cells are located (Figure 6D). Thus, the cellular architecture and pattern of chemokine expression in the MSs are different than in conventional lymphoid organs.

Milky Spots Support Somatic Hypermutation and Affinity Maturation

The lack of a well-defined conventional FDC network made us question whether B cells responding to antigen could be selected for high-affinity antigen receptors in the MSs. To test whether somatic hypermutation and affinity selection were occurring in the MSs of the omentum, we immunized WT and SLP mice with NP-OVA on day 0 and amplified NP-specific IgG1 heavy chain

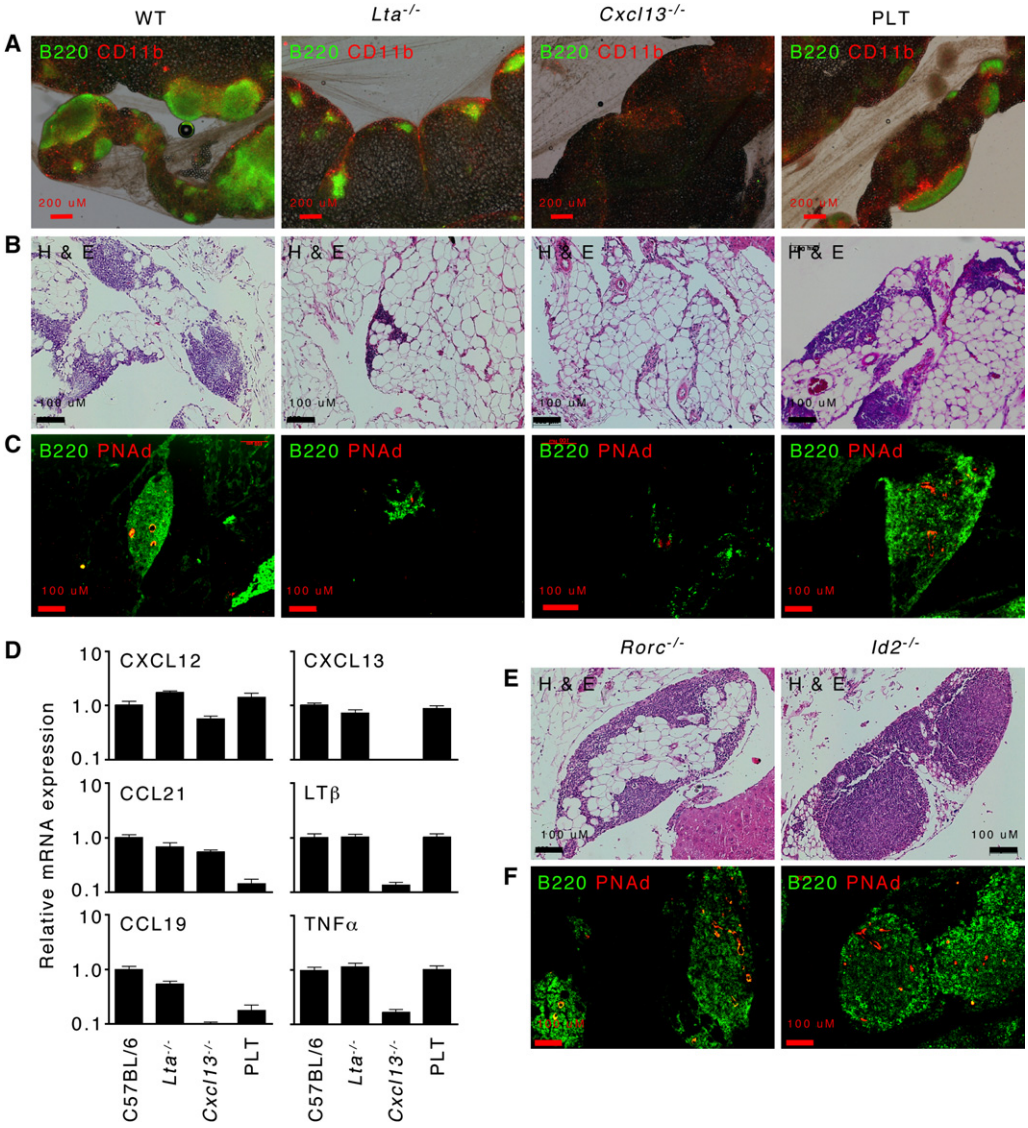

Figure 5. Milky Spot Development Requires LTα and CXCL13, but Not LTi Cells

(A) Omenta were obtained from naive C57BL/6, *Lta*$^{-/-}$, *Cxcl13*$^{-/-}$, or PLT mice as indicated and whole mounts were probed with antibodies to B220 and CD11b.

(B) Paraffin sections of omenta were stained with H&E.

(C) Paraffin sections of omenta were probed with antibodies to B220 and PNAd.

(D) RNA was extracted from the omenta of naive C57BL/6, *Lta*$^{-/-}$, *Cxcl13*$^{-/-}$, or PLT mice as indicated and assayed for the expression of CXCL12, CXCL13, CCL19, CCL21, LTβ, and TNF-α by quantitative PCR. The expression of each mRNA was normalized first to GAPDH and then normalized to the expression in WT animals, which was set at 1.

(E and F) Omenta were obtained from naive *Rorc*$^{-/-}$ or *Id2*$^{-/-}$ mice as indicated and paraffin sections were stained with H&E (E) or probed with antibodies to B220 and PNAd (F). Images are representative of 3–5 mice per group.

V regions by using primers specific for V186.2 and the IgG1 constant region on day 7, day 14, and day 19 (5 days after boosting) and sequenced individual clones. Although we observed only a few mutations in the V regions of IgG heavy chains from either WT or SLP mice on day 7, more sequences in both groups had accumulated mutations by days 14 and 19 after immunization (Figure 7A). However, more of the sequences from WT mice had mutations and the number of mutations in each V region was also higher in sequences from WT mice than those from SLP mice on days 14 and 19 (Figure 7A). Furthermore, 16/25 sequences from WT mice on day 14 exhibited the W to L mutation at position 33 that confers about a 10-fold higher affinity for NP (Figures S4A and S4B). In contrast, only 5/22 sequences from SLP mice exhibited this mutation at this time. Strikingly, 11/13 sequences from WT mice exhibited the W to L mutation at day 19, whereas 0/12 sequences from SLP mice had this mutation (Figures S4A and S4B). The differences in sequence were not limited to the patterns of mutations, as shown by the fact that 16/25 sequences from WT mice on day 14 had the YYYG motif at the V-D junction, which is characteristic of NP-binding

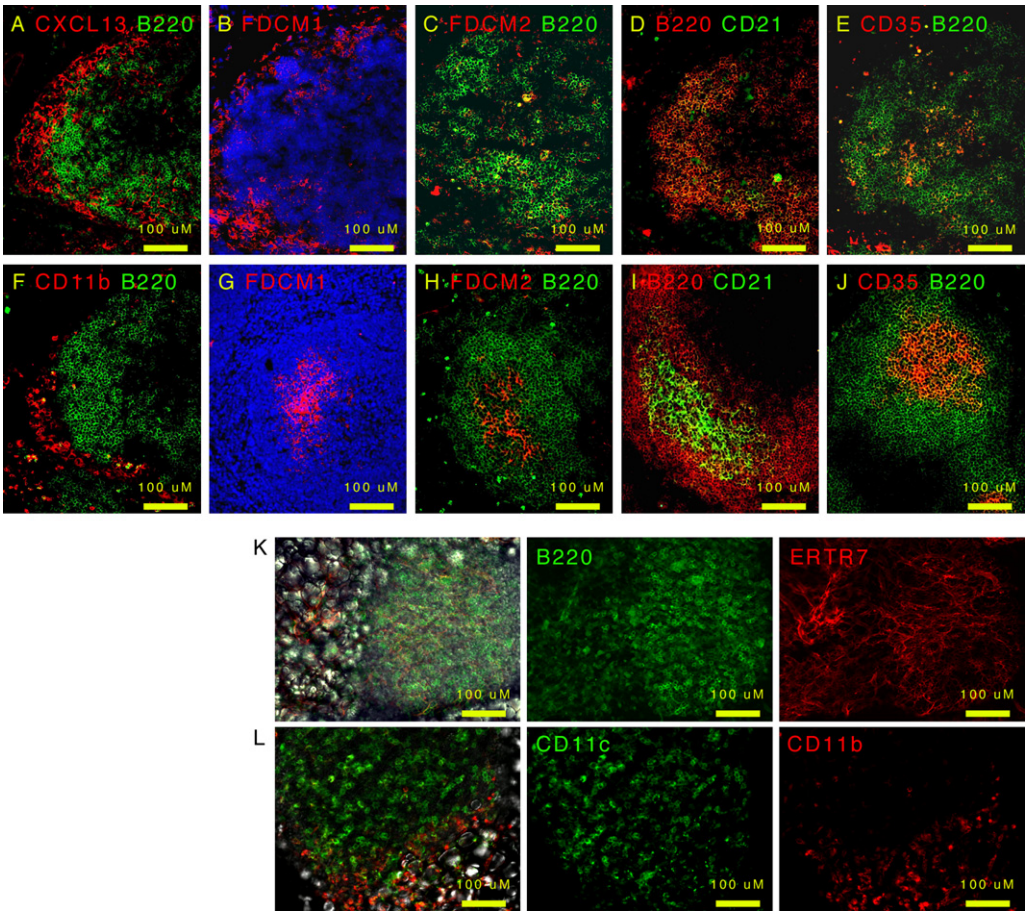

Figure 6. CXCL13 Is Expressed Surrounding the B Cell Areas

(A–F) Omenta were obtained from naive C57BL/6 mice and cryosections were probed with the indicated antibodies.

(G–J) Spleens were obtained from naive C57BL/6 mice and cryosections were probed with the indicated antibodies.

Cryosections in (B)–(E) were stained at the probed at the same time, under the same conditions as the corresponding cryosections in (G)–(J).

(K and L) Omenta were obtained from naive C57BL/6 mice and whole mounts were probed with the indicated antibodies. Images were generated by a combination of fluorescence (optical sections with the Zeiss apotome) and DIC. Control primary and secondary antibodies were negative. Images are representative of 3–5 mice.

sequences, whereas only 7/22 sequences from SLP mice had this motif. Interestingly, all of the W to L mutations in sequences from SLP mice were from those that contained the YYYG motif. Thus, although somatic hypermutation is still evident in SLP mice, the process of clonal selection seems to be very different.

To directly determine whether B cells responding to NP-OVA in the MSs underwent affinity maturation, we performed NP-specific ELISAs with plates coated with either NP_2BSA or NP_{16}BSA and compared the ratio of IgG that bound to each as a measure of the relative affinity of the antibody. As shown in Figure 7B, the affinity of NP-specific IgG from both WT and SLP mice was relatively low at day 10 after immunization. The affinity of NP-specific IgG increased rapidly in WT mice and increased somewhat more slowly in SLP mice (Figure 7B). Ultimately, however, the relative affinity of NP-specific IgG reached similar levels in both groups as measured in this assay. Together, these data demonstrate that the MSs of the omentum support some aspects of T cell-dependent B cell responses, although the process of clonal selection is unusual.

DISCUSSION

Previous work suggested that the omentum had an immunological function and showed that plasma cells could be found in the omentum after intraperitoneal immunization with T cell-independent antigens (Ansel et al., 2002; Ha et al., 2006) as well as classic T cell-dependent antigens (Dux et al., 1977; Hajdu et al., 1972; Van Vugt et al., 1996). Nevertheless, some authors conclude that the MSs should not be classified as secondary lymphoid organs (Szaniawska, 1974, 1975; Van Vugt et al., 1996). Given the lack of FDC networks in MSs (Van Vugt et al., 1996), the prevalence of B1 cells in the peritoneal cavity and omentum (Ansel et al., 2002), and the altered repertoire and affinity selection of B cells responding to antigen in the MSs of mice that lack conventional lymphoid organs, we would agree with Van Vugt et al. (1996) that the MSs are not conventional secondary lymphoid organs. However, Van Vugt's conclusion that they should rather be classified as perivascular infiltrates is, in our opinion, too limiting. Our data clearly show that the MSs of the omentum are

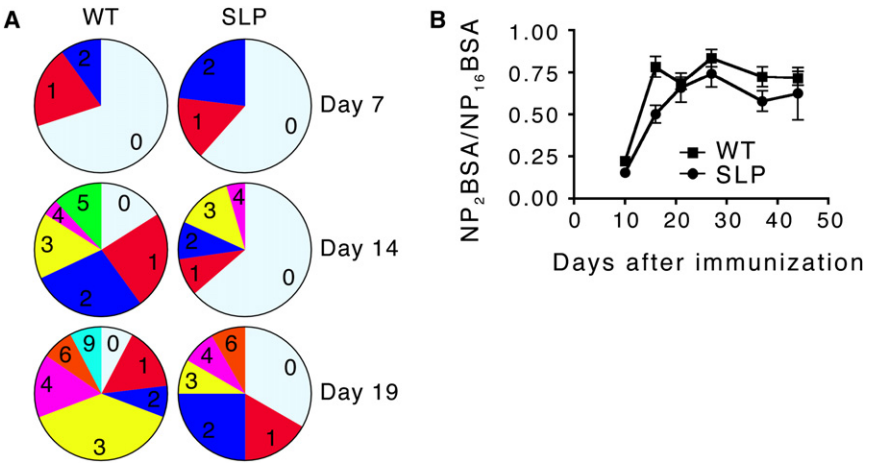

Figure 7. Somatic Hypermutation and Affinity Selection Occurs in the Absence of Conventional Secondary Lymphoid Organs

(A) WT and SLP mice were i.p. immunized with NP-OVA and boosted on day 14. RNA was extracted from omenta on days 7, 14, and 19 after immunization. The V regions of B cells with V186.2 heavy chains that had switched to IgG1 were amplified by PCR, subcloned, and sequenced. The pie charts indicate the relative proportion of sequences that were unmutated (0) or contained the indicated number of mutations.

(B) The titers of NP-specific total IgG were determined with ELISA plates coated with either NP_{16}-BSA or NP_2-BSA. The relative affinity of the NP-specific IgG is expressed as a ratio of binding to the NP_2-BSA versus NP_{16}-BSA. There were five mice in each group and this experiment is representative of three independent experiments.

present prior to immunization and support B cell responses (albeit unusual ones) as well as $CD4^+$ and $CD8^+$ T cell responses to antigens that are administered i.p. Moreover, B cells as well as $CD4^+$ and $CD8^+$ T cells primed in distal locations recirculate through the peritoneal cavity and omentum, indicating that the MSs of the omentum are sites of immune surveillance for a wide spectrum of antigens. Together, these data suggest that the omentum functions much more broadly as a secondary lymphoid organ than previously realized, even though it is structurally, developmentally, and functionally unique.

Unlike encapsulated LNs, which acquire antigen via afferent lymphatics, or mucosal lymphoid tissues, which transport antigen across mucosal epithelium, the MSs of the omentum open directly to the peritoneal cavity and collect cells and antigens suspended in the peritoneal fluid (Cui et al., 2002; Gerber et al., 2006; Hodel, 1970). Although LPS-activated peritoneal B1 cells use chemokine receptors to rapidly migrate to the MSs (Ha et al., 2006), i.p. administered naive B and T cells also collect in the MSs—even when treated with pertussis toxin, suggesting that at least some of the movement from the peritoneal cavity through the omentum occurs via bulk flow rather than specific homing. Consistent with this, free SRBCs in the peritoneal cavity can be collected in the omentum, although most are rapidly phagocytosed by macrophages and DCs. The presence of PNAd-expressing HEVs in the MSs also suggests that naive B and T cells can also be recruited to the MSs from the blood. In fact, a recent study shows that B2 cells use $\alpha4\beta7$-MAdCAM interactions to enter the MSs of the omentum from the blood (Berberich et al., 2008), and other studies show that fibronectin as well as various cell adhesion molecules are important for the entry and migration of peritoneal cells (Cui et al., 2002). Together, these data suggest a model in which recirculating T and B cells entering the MSs from the blood are confronted with a parade of antigens and cells from the peritoneal cavity, such as those released by abdominal surgery, peritoneal dialysis, peritoneal tumor metastases, and peritoneal infections. This intersection of recirculating lymphocytes and peritoneal drainage makes the MSs ideal sites for the initiation of local immune responses.

Unlike conventional lymphoid organs, which have B cell follicles arranged around networks of FDCs (Endres et al., 1999; Tew et al., 1997), the B cell areas of the MSs appear to lack central FDC networks and instead are surrounded by reticular networks of $CD11b^+$ and $FDCM1^+$ cells. Although CXCL13 is normally associated with a central reticular network in the B cell follicles of conventional lymphoid organs (Cyster et al., 2000), CXCL13 is expressed around the outside of the B cell areas of MSs in the same area that contains $CD11b^+$ cells. It is likely that the $CD11b^+$ cells are macrophages, which are known to express CXCL13 in the peritoneal cavity (Ansel et al., 2002), but it is unclear whether the $FDCM1^+$ cells are also macrophages, FDC precursors, or some other cell type. Given that other FDC markers do not stain in the same area and also do not detect a well-defined reticular network in the center of the B cell areas, it is difficult to make a firm conclusion regarding the status of FDCs in the omentum. However, the structure of the MSs seems inside-out relative to that of conventional lymphoid organs or even ectopic lymphoid follicles.

Despite the unusual architecture of the milky spots, we observe somatic hypermutation and some degree of affinity maturation in B cell responses from mice that lack conventional lymphoid organs, but retain MSs. Interestingly, the repertoire of V186.2 IgG heavy chains from the omenta of NP-OVA-immunized SLP mice contains some unusual features, such as a relative paucity of sequences with the YYYG motif at the V-D junction and very few sequences that encode the W to L mutation, despite the relatively robust accumulation of mutations overall. Although it is tempting to conclude that affinity maturation failed in these animals, the relative avidity for NP_2BSA does increase in SLP mice over the first 21 days after immunization, albeit more slowly than in WT mice. Unfortunately, the ELISA-based assay of relative affinity has a relatively narrow dynamic range and cannot differentiate between antibodies with affinities higher than about 10^{-7} M. Thus, the NP-specific antibodies generated in WT mice could ultimately have much higher affinities than those generated in SLP mice. Interestingly, the few sequences from SLP mice that acquired the W to L mutation all had the canonical YYYG motif at the V-D junction. Thus, an alternative explanation is that the initial repertoire of B cells recruited into the NP response is different in WT and SLP mice and that many of the heavy chains from SLP mice lacking the YYYG motif and the W to L substitution accumulate different mutations that also confer higher affinity for NP.

The difference in frequency of W to L substitutions between sequences from WT and SLP mice is also striking in another way. If we assume that the sequences obtained from SLP mice are typical of the V regions that are selected in the omentum, then the high frequency of B cells with the W to L mutation in WT mice must mean that those B cells were originally selected in other lymphoid organs and that their progeny recirculated back to the omentum. Because the sequences that have the W to L substitution vastly outnumber those that lack the W to L substitution in WT mice, this suggests that the clones that are selected in conventional lymphoid organs and recirculate to the omentum outcompete those clones that are selected in situ. If competitive fitness is determined by relative affinity (Dal Porto et al., 2002), then the B cells selected in conventional lymphoid organs containing the W to L substitution would be of higher affinity that those selected locally. If this were true, however, we should still observe in SLP mice an increase in the frequency of sequences with the W to L mutation between day 14 and 19 after immunization. The fact that we do not observe this increase means that clones with the W to L mutation are not selectively advantaged in SLP mice and that they are competing with clones of equivalent affinity or that affinity selection is not occurring. Although some degree of affinity maturation can occur in the absence of either germinal centers or immune complex deposition on FDCs (Hannum et al., 2000; Koni and Flavell, 1999) and can occur in the disorganized spleens of *Lta*$^{-/-}$ and *Ltbr*$^{-/-}$ mice (Futterer et al., 1998; Matsumoto et al., 1996a), it has long been assumed that immune complexes trapped on the surface of FDCs facilitate B cell selection and affinity maturation. Thus, the lack of clearly identifiable FDCs in MSs may contribute to poor affinity-based selection.

Unlike the development of the majority of secondary lymphoid organs, the development of the MSs occurs independently of RORγ-dependent or Id2-dependent LTi cells, suggesting that MSs use alternative cell types to trigger the differentiation of local mesenchymal cells into stromal cells that support lymphoid architecture. Of course the stromal elements in the MSs are very different than those in conventional lymphoid tissues, because the MSs lack clearly identifiable FDCs and maintain only an ERTR7^{+} stromal network. Another unusual feature of milky spot development and organization is the minimal role for LTα. Although the MSs are clearly compromised in the absence of LTα, their structure is completely restored in adult mice after reconstitution with *Lta*$^{+/+}$ hematopoietic cells, suggesting that the defects in the MSs of *Lta*$^{-/-}$ mice are due to nondevelopmental defect, such as the poor differentiation of HEVs (Browning et al., 2005). This is reminiscent of the nasal associated lymphoid tissue (NALT), which develops independently of LTα, but requires LTα to maintain normal architecture because of its ability to promote the expression of chemokines and trigger the differentiation of PNAd-expressing HEVs (Fukuyama et al., 2002; Harmsen et al., 2002; Rangel-Moreno et al., 2005). Surprisingly, however, the expression of homeostatic chemokines is normal in the omenta of *Lta*$^{-/-}$ mice, just like the induced expression of these chemokines in the lungs of *Lta*$^{-/-}$ mice during influenza infection (Moyron-Quiroz et al., 2004). However, despite the minimal role of LTα in the expression of CXCL13, CCL19, and CCL21, CXCL13 is very important for the development of the MSs. Essentially, no B cells are found in the omenta of *Cxcl13*$^{-/-}$ mice and the expression of CCL19, LTβ, and TNF-α is severely impaired (Ansel et al., 2002).

Taken altogether, these data demonstrate that the MSs of the omentum are unique secondary lymphoid organs that sample antigens from the peritoneal cavity and promote local, albeit unusual, immune responses. These results will be important for the understanding of how the omentum functions in response to antigens from abdominal surgeries, peritoneal dialysis, intestinal perforations, and even peritoneal tumor metastases.

EXPERIMENTAL PROCEDURES

Mice and Generation of Bone Marrow Chimeras

C57BL/6 mice and C57BL/6.129*Lta*^{tm1Dch} (*Lta*$^{-/-}$ mice) (de Togni et al., 1994) were obtained from the Jackson laboratory. *Cxcl13*$^{-/-}$ (Ansel et al., 2000) and PLT (Nakano et al., 1997) mice were a kind donation of J. Cyster (UCSF). *Rorc*$^{-/-}$ (Sun et al., 2000) and *Id2*$^{-/-}$ (Yokoto et al., 1999) mice were obtained from D. Littman (NYU). IL-4 reporter (4-get) mice (Mohrs et al., 2001) were obtained from M. Mohrs (Trudeau Institute). WT and SLP chimeric mice were generated by lethally irradiating C57BL/6 and splenectomized *Lta*$^{-/-}$ mice and reconstituting them with 1 × 10^{7} whole bone marrow cells from C57BL/6 mice as described (Moyron-Quiroz et al., 2004, 2006). Mice were irradiated with 1000 rads from a ^{137}Cs source at 93 rad/min in two doses. Mice were allowed to reconstitute for at least 6 weeks prior to immunization. All gene-targeted mice were on the C57BL/6 background and bred in the animal facility of Trudeau Institute. All procedures involving animals were approved by the Trudeau Institute Institutional Animal Care and Use Committee and were conducted according to the principles outlined by the National Research Council.

Immunization and Infection

Mice were immunized i.p. with 100 μg NP-OVA or 100 μg TNP-KLH adsorbed to alum or with 1 × 10^{6} SRBCs in PBS or with 100 μg Alexa-594-OVA. Mice were intranasally infected with 100 egg infectious units of A/PR8/34 influenza or orally infected with 200 *Heligmosomoides polygyrus* larvae.

Isolation of RNA, PCR, and Sequencing

RNA was extracted from whole omentum via an RNeasy kit (QIAGEN). 2 μg of DNase-treated RNA were reverse transcribed with random hexamers and Superscript II (Invitrogen). Quantitative PCR was performed with Taqman master mix, according to the Applied Biosystems protocol. Primers and probes for CXCL12, CXCL13, CCL19, LTβ, and TNF-α were obtained from Applied Biosystems. Primers for CCL21 (5′-AGACTCAGGAGCCCAAAGCA-3′ and 5′-GTTGAAGCAGGGCAAGGGT-3′) and GAPDH (5′CTCGTCCCGTAGA CAAAATGG-3′ and 5′-AATCTCCACTTTGCCACTGCA-3′) were synthesized by IDT. The probes for CCL21 (5′-FAM-CCACCTCATGCTGGCCTCCGT-BHQ-3′) and for GAPDH (5′-FAM-CGGATTTGGCCGTATTGGGCG-BHQ-3′) were synthesized by Biosearch Technology. The ABI Prism 7700 Taqman instrument was available through the molecular biology core facility at the Trudeau Institute. cDNAs of VH regions from NP-specific BCRs were amplified with a forward primer specific for V186.2 NP 5-1 CATGCTCTTCTTGGCAGC AACAGC and a reverse primer specific for IgG1 NP 3-1 GTGCACACCGCTGG ACAGGGATCC. PCR reactions were performed for 1 min at 94°C, 1.5 min at 58°C, and 2 min at 72°C for 25 cycles with Expand High-Fidelity Taq polymerase from Roche. The PCR product was cloned into TOPO vector (Invitrogen) and DNA from individual colonies was purified and sequenced. Sequencing was performed by Polymorphic DNA Technologies and sequence data was aligned with Sequencher software.

Cell Purification and Labeling

B cells, total T cells, and CD4^{+} T cells were purified by positive selection with MACS beads. For B cells and CD4^{+} T cells, anti-B220 or anti-CD4 magnetic beads (Miltenyi Biotec) were added directly to single-cell suspensions at 25 μl beads per 1 × 10^{8} total cells in 100 μl final volume and incubated on ice for an additional 15 min on ice. For total T cells, cells were first incubated with biotinylated anti-CD4 and anti-CD8 followed by streptavidin magnetic beads (Miltenyi Biotec). Cells were washed, filtered, and passed over a type LS^{+} magnetic column (Miltenyi Biotec). After washing, the magnetically bound cells were eluted from the column with the supplied plunger. Purified OTII CD4^{+} T cells were labeled with 5 μM carboxyfluoroscein succinimidyl ester

(CFSE) in PBS for 10 min at 37°C. Total T cells were labeled with 0.2 μM 4, 4 difluoro-5(2thienyl)-4-bora-3a, 4a-diaza-s-indacene-3-propionic acid, succinimidyl ester (BODIPY 558/568) in PBS for 10 min at 37°C. In some cases, cells were incubated at 3×10^7/ml with 100 ng/ml pertussis toxin for 2 hr at 37°C in complete RPMI with 2% FBS, 10 mM HEPES, 2 mM glutamine, 100 μg/ml streptomycin, and 100 U/ml penicillin.

Flow Cytometry

Omenta were digested with Collagenase D (Roche) at 37°C for 1 hr and mechanically disrupted by passage through a wire mesh, and live leukocytes were obtained by density gradient centrifugation with Lympholyte-Poly (Cedarlane). Fc receptors were blocked with 10 μg/ml 2.4G2, followed by staining with antibodies or MHC class I tetramers. The H-$2D^b$ class I tetramer containing $NP_{366-374}$ peptide were generated by the Trudeau Institute Molecular Biology Core Facility as described (Flynn et al., 1998; Murali-Krishna et al., 1998). NP-specific B cells were identified with NP-allophycocyanin (NP-APC). Fluorochrome-labeled antibodies to CD8, CD4, CD62L, CD138, FAS, and CD19 were obtained from BD Biosciences. FITC-labeled PNA was obtained from Sigma.

ELISAs and ELISPOTs

Plates were coated with $NP_{(16)}$-BSA, $NP_{(2)}$-BSA, or $TNP_{(5)}$-BSA at 1 μg/ml and blocked with 10 mg/ml BSA. Serum samples were initially diluted 100-fold in PBS with 10 mg/ml BSA and 0.1% Tween-20 and then serially diluted in 3-fold steps in the same buffer and applied to the coated plates. Bound Ig was detected with horseradish peroxidase-conjugated goat anti-mouse IgM or goat anti-mouse IgG from Southern Biotechnology Associates. IgG1, IgG2a, IgG2b, and IgG3 were detected with HRP-conjugated isotype-specific antibodies from BD Biosciences. Purified monoclonal TNP antibodies (A111-3 and G155-178 BD Biosciences) were used as standards for the anti-TNP ELISAs. Antibody titers are defined as the dilution required to reduce a positive signal to 3-fold above background. ELISPOTs were performed as described (Rangel-Moreno et al., 2005).

Immunofluorescence

Whole omenta were placed in 24-well plates and blocked with 10 μg/ml 2.4G2 in PBS with 5% BSA for 1 hr at 4°C while rocking. Fluorochrome-conjugated antibodies were then added for an additional 4 hr at 4°C while rocking. Omentums were washed 3 times for 15 min each in PBS with 5% BSA and then wet mounted in PBS with 5% BSA. Omenta were also prepared for histology by folding strips of omentum into a piece of liver, fixing the tissue with 10% neutral buffered formalin, and embedding in paraffin. Paraffin sections were treated with Antigen Retrieval Solution (DAKO) at 96°C for 20 min and then cooled at room temperature for 20 min before blocking and staining as described above. Sections probed with fluorescent antibodies were counterstained with DAPI. Cryosections were obtained by cutting tissues in the presence of dry ice so that the fatty tissue of the omentum could be cut. All tissues were viewed with a Zeiss Axiovert 200 m microscope with Apotome. Green and red fluorescence was captured with appropriate filter sets and in some cases, combined with images obtained with DIC. Some images were obtained as optical sections with the Apotome. Images were recorded with a Zeiss AxioCam digital camera with Zeiss AxioVision 4.5 software and saved as TIFF files. Antibodies to CD21, CD11b, CD11C, B220, CD35, and PNAd were obtained from BD Biosciences and conjugated to either Alexa Fluor 488 or Alexa Fluor with kits from Invitrogen. Purified goat anti-mouse CXCL13 (R&D Systems) was detected with Alexa Fluor 594-conjugated donkey anti-goat IgG (Molecular Probes).

SUPPLEMENTAL DATA

Supplemental Data include four figures and can be found with this article online at http://www.cell.com/immunity/supplemental/S1074-7613(09)00186-1.

ACKNOWLEDGMENTS

The authors would like to thank F. Lund for helpful discussions during the course of this work and M. Tighe for help with histology and microscopy. This work was supported by the Trudeau Institute and NIH grants HL69409, AI072689, and AI061511.

Received: June 18, 2007
Revised: September 16, 2008
Accepted: March 6, 2009
Published online: May 7, 2009

REFERENCES

Ansel, K.M., Ngo, V.N., Hayman, P.L., Luther, S.A., Forster, R., Sedgwick, J.D., Browning, J.L., Lipp, M., and Cyster, J.G. (2000). A chemokine-driven positive feedback loop organizes lymphoid follicles. Nature *406*, 309–314.

Ansel, K.M., Harris, R.B., and Cyster, J.G. (2002). CXCL13 is required for B1 cell homing, natural antibody production, and body cavity immunity. Immunity *16*, 67–76.

Banks, T.A., Rouse, B.T., Kerley, M.K., Blair, P.J., Godfrey, V.L., Kuklin, N.A., Bouley, D.M., Thomas, J., Kanangat, S., and Mucenski, M.L. (1995). Lymphotoxin a deficient mice: effects on secondary lymphoid organ development and humoral immune responsiveness. J. Immunol. *155*, 1685–1693.

Beelen, R.H., Fluitsma, D.M., and Hoefsmit, E.C. (1980). The cellular composition of omentum milky spots and the ultrastructure of milky spot macrophages and reticulum cells. J. Reticuloendothel. Soc. *28*, 585–599.

Beelen, R.H., Oosterling, S.J., van Egmond, M., van den Born, J., and Zareie, M. (2005). Omental milky spots in peritoneal pathophysiology (spots before your eyes). Perit. Dial. Int. *25*, 30–32.

Benedict, C.L., and Kearney, J.F. (1999). Increased junctional diversity in fetal B cells results in a loss of protective anti-phosphorylcholine antibodies in adult mice. Immunity *10*, 607–617.

Berberich, S., Dahne, S., Schippers, A., Peters, T., Muller, W., Kremmer, E., Forster, R., and Pabst, O. (2008). Differential molecular and anatomical basis for B cell migration into the peritoneal cavity and omental milky spots. J. Immunol. *180*, 2196–2203.

Browning, J.L., Allaire, N., Ngam-Ek, A., Notidis, E., Hunt, J., Perrin, S., and Fava, R.A. (2005). Lymphotoxin-beta receptor signaling is required for the homeostatic control of HEV differentiation and function. Immunity *23*, 539–550.

Cattoretti, G., Chang, C.C., Cechova, K., Zhang, J., Ye, B.H., Falini, B., Louie, D.C., Offit, K., Chaganti, R.S., and Dalla-Favera, R. (1995). BCL-6 protein is expressed in germinal-center B cells. Blood *86*, 45–53.

Cui, L., Johkura, K., Liang, Y., Teng, R., Ogiwara, N., Okouchi, Y., Asanuma, K., and Sasaki, K. (2002). Biodefense function of omental milky spots through cell adhesion molecules and leukocyte proliferation. Cell Tissue Res. *310*, 321–330.

Cyster, J.G., Ansel, K.M., Rief, K., Hyman, P.L., Tang, H.L., Luther, S.A., and Ngo, V.N. (2000). Foliicular stromal cells and lymphocyte homing to follicles. Immunol. Rev. *176*, 181–193.

Dal Porto, J.M., Haberman, A.M., Kelsoe, G., and Shlomchik, M.J. (2002). Very low affinity B cells form germinal centers, become memory B cells, and participate in secondary immune responses when higher affinity competition is reduced. J. Exp. Med. *195*, 1215–1221.

Das, S.K. (1976). The size of the human omentum and methods of lengthening it for transplantation. Br. J. Plast. Surg. *29*, 170–244.

de Togni, P., Goellner, J., Ruddle, N.H., Streeter, P.R., Fick, A., Mariathasan, S., Smith, S.C., Carlson, R., Shornick, L.P., Strauss-Schoenberger, J., et al. (1994). Abnormal development of peripheral lymphoid organs in mice deficient in lymphotoxin. Science *264*, 703–707.

Di Paolo, N., Sacchi, G., Garosi, G., Sansoni, E., Bargagli, L., Ponzo, P., Tanganelli, P., and Gaggiotti, E. (2005). Omental milky spots and peritoneal dialysis—review and personal experience. Perit. Dial. Int. *25*, 48–57.

Dux, K., Janik, P., and Szaniawska, B. (1977). Kinetics of proliferation, cell differentiation and IgM secretion in the omental lymphoid organ of B10/Sn mice following intraperitoneal immunization with sheep erythrocytes. Cell. Immunol. *32*, 97–109.

Dux, K., Rouse, R.V., and Kyewski, B. (1986). Composition of the lymphoid cell populations from omental milky spots during the immune response in C57BL/Ka mice. Eur. J. Immunol. *16*, 1029–1032.

Endres, R., Alimzhanov, M.B., Plitz, T., Futterer, A., Kosco-Vilbois, M.H., Nedospasov, S.A., Rajewski, K., and Pfeffer, K. (1999). Mature follicular

dendritic cell networks depend on expression of lymphotoxin b receptor by radioresistant stromal cells and of lymphotoxin b and tumor necrosis factor by B cells. J. Exp. Med. *189*, 159–167.

Fedorko, M.E., Hirsch, J.G., and Fried, B. (1971). Studies on transport of macromolecules and small particles across mesothelial cells of the mouse omentum. II. Kinetic features and metabolic requirements. Exp. Cell Res. *69*, 313–323.

Flynn, K.J., Belz, G.T., Altman, J.D., Ahmed, R., Woodland, D.L., and Doherty, P.C. (1998). Virus-specific CD8+ T cells in primary and secondary influenza pneumonia. Immunity *8*, 683–691.

Fukuyama, S., Hiroi, T., Yokota, Y., Rennert, P.D., Yanagita, M., Kinoshita, N., Terawaki, S., Shikina, T., Yamamoto, M., Kurono, Y., and Kiyono, H. (2002). Initiation of NALT organogenesis is independent of the IL-7R, LTbetaR, and NIK signaling pathways but requires the Id2 gene and CD3(-)CD4(+)CD45(+) cells. Immunity *17*, 31–40.

Futterer, A., Mink, K., Luz, A., Kosco-Vilbois, M.H., and Pfeffer, K. (1998). The lymphotoxin b receptor controls organogenisis and affinity maturation in peripheral lymphoid tissues. Immunity *9*, 59–70.

Gerber, S.A., Rybalko, V.Y., Bigelow, C.E., Lugade, A.A., Foster, T.H., Frelinger, J.G., and Lord, E.M. (2006). Preferential attachment of peritoneal tumor metastases to omental immune aggregates and possible role of a unique vascular microenvironment in metastatic survival and growth. Am. J. Pathol. *169*, 1739–1752.

Goldsmith, H.S., Griffith, A.L., Kupferman, A., and Catsimpoolas, N. (1984). Lipid angiogenic factor from omentum. JAMA *252*, 2034–2036.

Ha, S.A., Tsuji, M., Suzuki, K., Meek, B., Yasuda, N., Kaisho, T., and Fagarasan, S. (2006). Regulation of B1 cell migration by signals through Toll-like receptors. J. Exp. Med. *203*, 2541–2550.

Hajdu, I., Holub, M., and Trebichavsky, I. (1972). The sequence of appearance of antibodies in mouse omentum plasma cells. Exp. Cell Res. *75*, 219–230.

Hannum, L.G., Haberman, A.M., Anderson, S.M., and Shlomchik, M.J. (2000). Germinal center initiation, variable gene region hypermutation, and mutant B cell selection without detectable immune complexes on follicular dendritic cells. J. Exp. Med. *192*, 931–942.

Harmsen, A., Kusser, K., Hartson, L., Tighe, M., Sunshine, M.J., Sedgwick, J.D., Choi, Y., Littman, D.R., and Randall, T.D. (2002). Organogenesis of nasal associated lymphoid tissue (NALT) occurs independently of lymphotoxin-α (LTα) and retinoic acid receptor-related orphan receptor-γ, but the organization of NALT is LTα-dependent. J. Immunol. *168*, 986–990.

Hodel, C. (1970). Ultrastructural studies on the absorption of protein markers by the greater omentum. Eur. Surg. Res. *2*, 435–449.

Koni, P.A., and Flavell, R.A. (1999). Lymph node germinal centers form in the absence of follicular dendritic cells networks. J. Exp. Med. *189*, 855–864.

Krist, L.F., Eestermans, I.L., Steenbergen, J.J., Hoefsmit, E.C., Cuesta, M.A., Meyer, S., and Beelen, R.H. (1995a). Cellular composition of milky spots in the human greater omentum: an immunochemical and ultrastructural study. Anat. Rec. *241*, 163–174.

Krist, L.F., Kerremans, M., Koenen, H., Blijleven, N., Eestermans, I.L., Calame, W., Meyer, S., and Beelen, R.H. (1995b). Novel isolation and purification method permitting functional cytotoxicity studies of macrophages from milky spots in the greater omentum. J. Immunol. Methods *184*, 253–261.

Krist, L.F., Kerremans, M., Broekhuis-Fluitsma, D.M., Eestermans, I.L., Meyer, S., and Beelen, R.H. (1998). Milky spots in the greater omentum are predominant sites of local tumour cell proliferation and accumulation in the peritoneal cavity. Cancer Immunol. Immunother. *47*, 205–212.

Matsumoto, M., Lo, S.F., Carruthers, C.J.L., Min, J., Mariathasan, S., Huang, G., Plas, D.R., Martin, S.M., Geha, R.S., Nahm, M.H., and Chaplin, D.D. (1996a). Affinity maturation without germinal centers in lymphotoxin a deficient mice. Nature *382*, 462–466.

Matsumoto, M., Mariathasan, S., Nahm, M.H., Baranyay, F., Peschon, J.J., and Chaplin, D.D. (1996b). Role of lymphotoxin and the type 1 TNF receptor in the formation of germinal centers. Science *271*, 1289–1291.

Mohrs, M., Shinkai, K., Mohrs, K., and Locksley, R.M. (2001). Analysis of type 2 immunity in vivo with a bicistronic IL-4 reporter. Immunity *15*, 303–311.

Morrison, R. (1906). On the functional aspects of the greater omentum. BMJ *1*, 76–78.

Moyron-Quiroz, J.E., Rangel-Moreno, J., Kusser, K., Hartson, L., Sprague, F., Goodrich, S., Woodland, D.L., Lund, F.E., and Randall, T.D. (2004). Role of inducible bronchus associated lymphoid tissue (iBALT) in respiratory immunity. Nat. Med. *10*, 927–934.

Moyron-Quiroz, J.E., Rangel-Moreno, J., Hartson, L., Kusser, K., Tighe, M.P., Klonowski, K.D., Lefrancois, L., Cauley, L.S., Harmsen, A.G., Lund, F.E., and Randall, T.D. (2006). Persistence and responsiveness of immunologic memory in the absence of secondary lymphoid organs. Immunity *25*, 643–654.

Murali-Krishna, K., Altman, J.D., Suresh, M., Sourdive, D.J., Zajac, A.J., Miller, J.D., Slansky, J., and Ahmed, R. (1998). Counting antigen-specific CD8 T cells: A reevaluation of bystander activation during viral infection. Immunity *8*, 177–187.

Nakano, H., and Gunn, M.D. (2001). Gene duplications at the chemokine locus on mouse chromosome 4: Multiple strain-specific haplotypes and the deletion of secondary lymphoid-organ chemokine and EBI-1 ligand chemokine genes in the plt mutation. J. Immunol. *166*, 361–369.

Nakano, H., Tamura, T., Yoshimoto, T., Yagita, H., Miyasaka, M., Butcher, E.C., Nariuchi, H., Kakiuchi, T., and Matsuzawa, A. (1997). Genetic defect in T lymphocyte-specific homing into peripheral lymph nodes. Eur. J. Immunol. *27*, 215–221.

Portis, B. (1924). Role of omentum of rabbits, dogs and guinea-pigs in antibody production. J. Infect. Dis. *34*, 159–185.

Rangel-Moreno, J., Moyron-Quiroz, J., Kusser, K., Hartson, L., Nakano, H., and Randall, T.D. (2005). Role of CXC chemokine ligand 13, CC chemokine ligand (CCL) 19, and CCL21 in the organization and function of nasal-associated lymphoid tissue. J. Immunol. *175*, 4904–4913.

Roberts, K.B. (1955). Antibody formation in the omentum. Br. J. Exp. Pathol. *36*, 357–362.

Solvason, N., and Kearney, J.F. (1992). The human fetal omentum: A site of B cell generation. J. Exp. Med. *175*, 397–404.

Solvason, N., Chen, X., Shu, F., and Kearney, J.F. (1992). The fetal omentum in mice and humans. A site enriched for precursors of CD5 B cells early in development. Ann. N Y Acad. Sci. *651*, 10–20.

Sun, Z., Unutmaz, D., Zou, Y.-R., Sunshine, M.J., Pierani, A., Brenner-Morton, S., Mebius, R.E., and Littman, D.R. (2000). Requirement for RORg in thymocyte survival and lymphoid organ development. Science *288*, 2369–2373.

Szaniawska, B. (1974). Changes in the greater omentum of mice of different strains after intraperitoneal immunization with sheep erythrocytes. I. Production of IgM immunoglobulins in milky spots. Arch. Immunol. Ther. Exp. (Warsz.) *22*, 585–593.

Szaniawska, B. (1975). Changes in the greater omentum of mice of different strains following intraperitoneal strains following intraperitoneal immunization with sheep erythrocytes. III. Determination of the percentage of thymus-dependent cells in the omental milky spots in mice by the application of anti-o serum. Arch. Immunol. Ther. Exp. (Warsz.) *23*, 19–24.

Tew, J.G., Wu, J., Qin, D., Helm, S., Burton, G.F., and Szakal, A.K. (1997). Follicular dendritic cells and presentation of antigen and costimulatory signals to B cells. Immunol. Rev. *156*, 39–52.

Vakil, M., Briles, D.E., and Kearney, J.F. (1991). Antigen-independent selection of T15 idiotype during B-cell ontogeny in mice. Dev. Immunol. *1*, 203–212.

Van Vugt, E., Van Rijthoven, E.A., Kamperdijk, E.W., and Beelen, R.H. (1996). Omental milky spots in the local immune response in the peritoneal cavity of rats. Anat. Rec. *244*, 235–245.

Walker, F.C., and Rogers, A.W. (1961). The greater omentum as a site of antibody synthesis. Br. J. Exp. Pathol. *42*, 222–231.

Williams, R., and White, H. (1986). The greater omentum: Its applicability to cancer surgery and cancer therapy. Curr. Probl. Surg. *23*, 789–865.

Yokoto, Y., Mansouri, A., Mori, S., Sugawara, S., Adachi, S., Nishikawa, S.I., and Gruss, P. (1999). Development of peripheral lymphoid organs and natual killer cells depends on the helix-loop-helix inhibitor Id2. Nature *397*, 702–706.